LHC Project Note 361

2005-02-21

Luca.Bottura@cern.ch

Scaling Laws for the Field Quality at Injection in the LHC Dipoles

L. Bottura, T. Pieloni, N. Sammut / Accelerator Technology Department

Keywords: Field Harmonics, Dynamic Effects, Scaling Law, Multipoles Factory, Reference Magnet System

Summary

The selection and use of reference magnets as a mean to improve predictability and reproducibility of the operation of the LHC depends on whether few magnets can be found that represent the average behavior of a sector, or, in the limit, of the whole accelerator. The purpose of this note is to show that it is possible to select magnets that represent well, on average, a family in the population of the magnets produced so far. We refer to this property by saying that the behavior of a single magnet can be scaled to be equal to the average of a family of magnets. The procedure used to achieve this equivalence is referred to as the scaling law.

Introduction

The experience accumulated in the three major operating superconducting accelerators, Tevatron, HERA and RHIC, shows that after commissioning there is a constant need for improving the knowledge of the magnetic state of the machine. This is done, most of the time, by direct beam measurements during Machine Development time. In complement to this, the experience that can be gained using off-line, dedicated magnetic measurements of magnets taken as a reference to the machine is extremely valuable to establish expected behaviours. One such example is given by the recent study of the sextupole in the Tevatron dipoles [1], [2]. Evidently, one needs here to make an implicit assumption that single magnets are representative of the whole accelerator. We refer to this property by saying that the behavior of a single magnet can be *scaled* to be equal to the average of a family of magnets. The procedure used to achieve this equivalence is referred to as the *scaling law*.

The main purpose of this report is to verify the scaling property for the LHC magnets. Most of the difficulties for the LHC operation are expected during injection and in the initial phase of the beam acceleration, during snap-back, where the reproducibility of the magnetic state is, to some extent, unknown. This report focusses on the search for a scaling law for the main field and field errors at injection. Furthermore, the scope of the study is limited to the dipoles, for which a relevant sample has been measured and statistics have been established. We finally further restrict the attention to the first allowed multipoles b1, b3 and b5, for which the effects are expected to be systematic. Where relevant, we will also quote results from other magnet productions, and in particular the experience at Fermilab on the Tevatron to which CERN has participated actively, and from the HERA reference magnets that have been extensively exploited to steer and optimise operation.

Scaling law for the time dependence of decay

LHC dipoles

The standard magnetic measurements executed on dipoles include a simulation of a 1000 s injection at 450 GeV after 30 minutes operation at 7 TeV. The field is measured during the injection porch. To verify the scalability of the behavior of a single magnet we have selected randomly 30 magnets from the present production, equally distributed among manufacturers. The list of magnets is given in Table 1, and Figs. 1, 2 and 3 report the variation of b_1, b_3 and b_5 during injection in both apertures of the magnet sample, arbitrarily shifted along the vertical axis to make the initial value at injection equal to zero.

Table 1. Magnets considered in the analysis of the dynamics of decay at injection

magnet	aperture		magnet	aperture		magnet	aperture	
	1	2		1	2		1	2
1008	x	x	2004	x	x	3008	x	x
1010	x	x	2007	x	x	3011	x	x
1015	x	x	2008	x	x	3012	x	x
1021	x	x	2010	x	x	3027	x	x
1027	x	x	2026	x	x	3034	x	x
1039	x	x	2027	x	x	3065	x	x
1043	x	x	2029	x	x	3070	x	x
1052	x	x	2046	x	x	3082		x
1063	x	x	2054	x	x	3083	x	x
			2060	x	x	3090	x	x
						3122	x	x

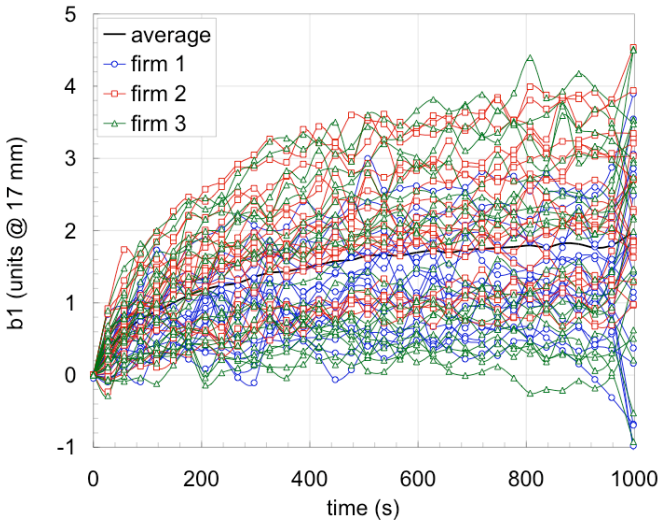

Figure 1. Decay of the normal dipole b_1 in the magnets of Tab. 1, measured during a 1000 s simulated injection porch following a standard cleansing cycle. The values have been arbitrarily shifted along the y axis to cancel the initial value of b_1.

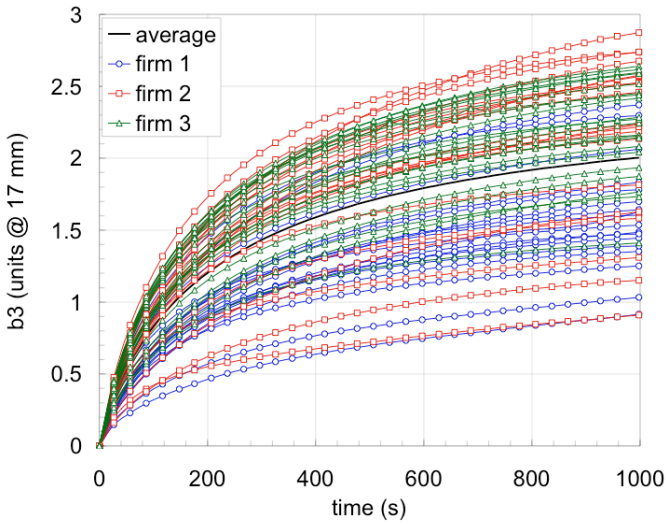

Figure 2. Decay of the normal sextupole b_3 in the magnets of Tab. 1, measured during a 1000 s simulated injection porch following a standard cleansing cycle. The values have been arbitrarily shifted along the y axis to cancel the initial value of b_3.

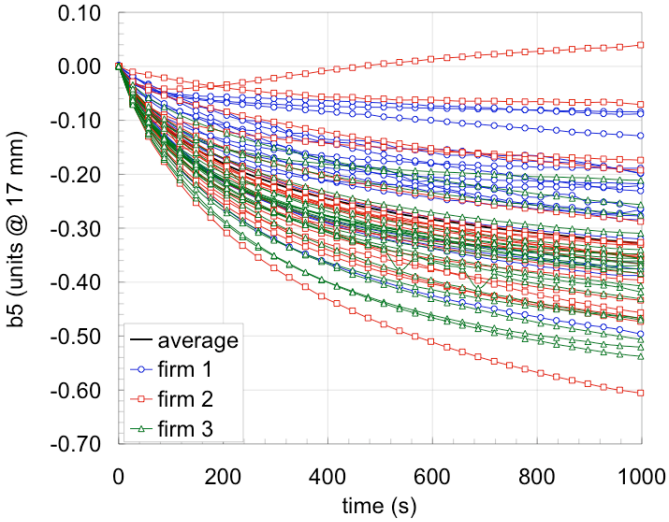

Figure 3. Decay of the normal decapole b_5 in the magnets of Tab. 1, measured during a 1000 s simulated injection porch following a standard cleansing cycle. The values have been arbitrarily shifted along the y axis to cancel the initial value of b_5.

From the data reported there we have computed the average decay at injection over this limited but significant population. The values obtained for the average and the r.m.s. after a 1000 s injection, are broadly consistent with the average and r.m.s. observed on the whole set of magnets cold measured to date. We can hence safely assume that the averages reported in the plots of Figs. 1, 2 and 3 represent an estimate of the average decay in the machine.

We have modeled the average decay as a function of time t using the following double exponential equation, with a fast decay with time constant τ_1 followed by a slower relaxation with time constant τ_2:

$$c_n^{decay} = \Delta_n \left[a^{\Delta} \left(1 - e^{-\frac{t-t_{inj}}{\tau_1}} \right) + \left(1 - a^{\Delta} \right) \left(1 - e^{-\frac{t-t_{inj}}{\tau_2}} \right) \right] \quad (1)$$

where we have taken the following constraint:

$$\tau_1 = \frac{\tau_2}{9} \quad (2)$$

that is justified by the interpretation of the decay as the consequence of current diffusion in the cables[1]. In addition, the exponential time constants have been taken equal for the analysis of the decay of all three harmonics, making the hypothesis that the dynamics is the same on all harmonics. Injection starts at time t_{inj}, the parameter Δ_n represents the asymptotic decay at the end of an ideal, infinitely long injection, and the parameter a^{Δ} gives the normalized weight of the fast component of the decay, and its complement to one, 1- a^{Δ}, is the weight of the slow component. The values of the parameters obtained as a result of the fits of the average decay are reported in Tab. 2, as well as the standard deviation of the difference between the sample average and the model. In all cases this last is of the order of 0.01 units @ 17 mm or smaller, which is sufficient for the further analysis.

parameter	units	b_1	b_3	b_5
τ_1	(s)	30	30	30
τ_2	(s)	270	270	270
a_Δ	(-)	0.20	0.15	0.09
Δ_n	(units @ 17 mm)	1.85	1.99	-0.32
fit σ	(units @ 17 mm)	0.013	0.014	0.004

Table 2. Parameters obtained fitting the model of Eq. (1) to the average decay in the population analyzed, representing the behavior of the LHC.

The most important matter is now to verify to which extent a single reference magnet can be chosen to represent the average behavior of the population. Observing the single magnet data, e.g. the normal sextupole b_3 of Fig. 2, it seems that a simple scaling factor applied to the decay of a single magnet could stretch the measured data in the y direction to match the average curve. This is clearly true if the dynamics of the decay does not change from magnet to magnet. Starting with this assumption, we have sought whether the scaling law:

$$\left\langle c_n^{decay} \right\rangle (t) = f_{decay} \; c_{n,i}^{decay}(t) \quad (3)$$

produces a satisfactory result. In Eq. (3) $\left\langle c_n^{decay} \right\rangle (t)$ is the average decay (i.e. the value for the sector or for the ring), $c_{n,i}^{decay}(t)$ is the decay of the reference magnet *i*, and f_{decay}

[1] Making the hypothesis that the cable current distributes continuously among the strands of a uniform cable, the time evolution of the currents is governed by an infinite series of harmonic modes damped by an exponential with time constants $\tau_n = \frac{\tau}{(2n-1)^2}$. In Eqs. (1) and (2) we have limited ourselves to the first two modes.

is the scaling factor. This last is determined as the ratio of the measured decays for the sample average and for the reference magnet chosen at the end of the simulated injection, i.e. in the above notation:

$$f_{decay} = \frac{\left\langle c_n^{decay} \right\rangle (t = 1000)}{c_{n,i}^{decay} (t = 1000)} \qquad (4).$$

We note here that there is no free parameter in the above scaling, all quantities being known once the magnets, or a suitable sample, have been measured in cold conditions.

We have used Eqs. (3) and (4) to scale the decay of each magnet measured, producing curves of the type represented in Fig. 4 for the normal sextupole of a selected magnet (in this case aperture 1 of dipole 1015). We have then computed the difference between the scaled decay and the average of the magnet population at all times during the injection porch. To quantify the goodness of the scaling we have finally sought the maximum of the absolute value of this difference.

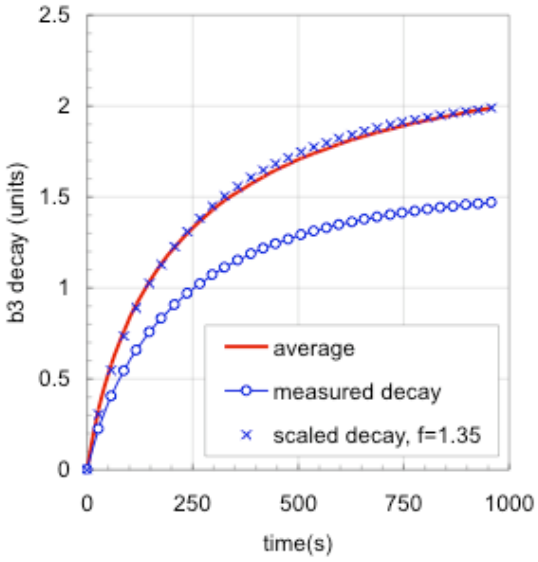

Figure 4. Example of scaling and comparison of scaled sextupole decays in magnet 1015, aperture 1.

The results for all magnets are summarised in the hystograms of Figs. 5, 6 and 7 for b_1, b_3 and b_5 respectively. The scaling law tested produces typical maximum scaling errors in the range 0.5 to 5 units @ 17 mm for b_1, 0.01 to 0.2 units @ 17 mm for b_3, and 0.05 to 0.1 units @ 17 mm for b_5. In the hystograms there are few outliers, generally related to magnets that have large scaling factor or anomalous behavior, appearing as a tail in the distributions. Because the hystograms are skewed, the most probable errors (the *mode* in the hystograms) are different, typically a factor 3 smaller, than the *medians* of the distribution. We make a conservative choice and take the medians as an indication for the typical error in a reference magnet selected at random, i.e. 0.85 units @ 17 mm for b_1, 0.08 units @ 17 mm for b_3 and 0.03 units @ 17 mm for b_5. In fact,

it would be in principle possible to achieve better results by selecting magnets based on their scaling error, and defining the scaling factor based on a general optimization in the time span available from measured data. This is not done here to keep the reasoning simple, and as it has little influence on the final conclusions.

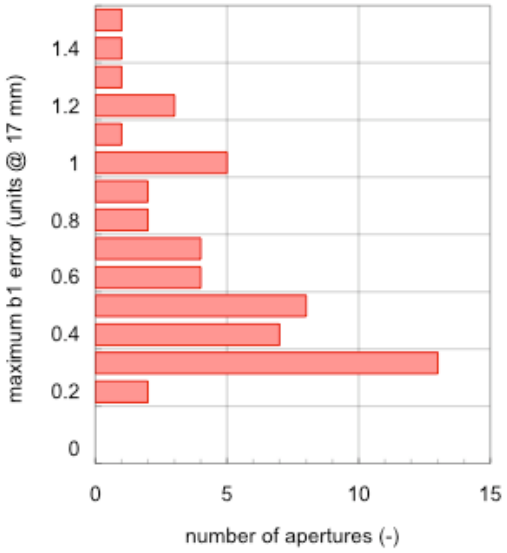

Figure 5. Histogram of the maximum difference between the scaled dipole decay and the average dipole decay of the magnet set analyzed.

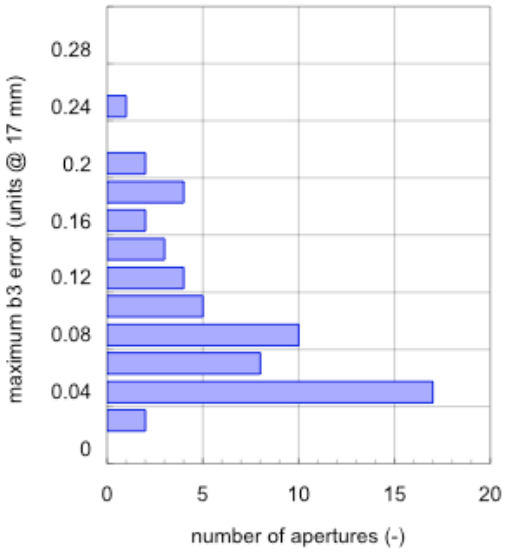

Figure 6. Histogram of the maximum difference between the scaled sextupole decay and the average sextupole decay of the magnet set analyzed.

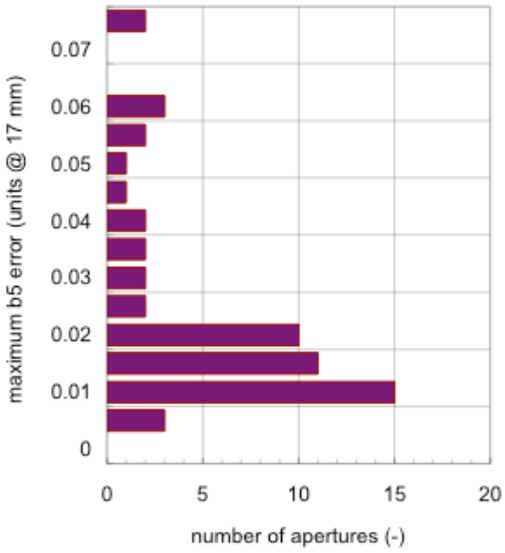

Figure 7. Histogram of the maximum difference between the scaled decapole decay and the average decapole decay of the magnet set analyzed.

Tevatron dipoles

As a part of the overall optimization of the Tevatron Run II, several dipole magnets were re-measured at the Magnet Test Facility in Fermilab [3], [4] aiming at reducing beam losses associated residual correction errors during injection and snap-back. Thanks to the copious results obtained in this measurement campaign, it was possible to compare the behavior of the sextupole during injection in specific magnets to the chromaticity measurements taken during the injection porch in the accelerator [2]. The result of this test is shown in Fig. 8, and it demonstrates that the good agreement between the average behavior of a magnet population and the scaled results from a single magnet is not accidental.

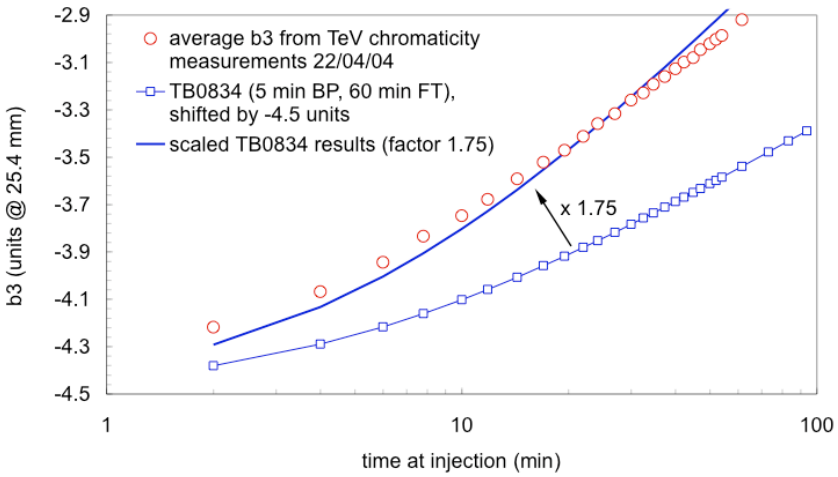

Figure 8. Comparison of the sextupole deduced from chromaticity measurement during an injection at Tevatron, and the scaled measurements in a spare dipole. Data by courtesy of P. Bauer, FNAL. The scaling factor was optimized to minimize the error over the complete injection porch, of 100 minutes.

In the case reported in Fig. 8 the scaled magnet behavior reproduces the dynamics of the Tevatron chromaticity evolution to within 0.04 units @ 25.4 mm over a time span of nearly 2 hours. This gives confidence that the scaling of Eq. (3) can produce results accurate enough for precise control.

HERA dipoles

The correction scheme employed by HERA at DESY makes use of on-line reference magnets and look up tables. Two reference magnets, one for each magnet production line, have been chosen to represent the behavior of the two halves of the proton ring. The reference magnets were chosen to be at the center of the drift spread of their respective magnet family. The reference magnets are powered in series with the magnet chain in the accelerator tunnel and are equipped with NMR and Hall probes, which measure the magnetic dipole field, a static pick-up coil, which is used to measure the ramping dipole field, and rotating coils for the sextupole contribution due to persistent current decay.

The fill of the 180 (3 x 60) proton bunches takes place at 40 GeV over a typical duration of 30 minutes. The beam parameters can be controlled automatically using the rotating coils in the reference magnets to measure the drift of the b_3 component, and using the NMR to detect the b_1 change [5]. The corrections obtained are applied without scaling to the corrector magnets in the ring. This corresponds to the scaling procedure outlined above for the LHC magnets, where the scaling factor f_{decay} of the single magnet to the average of the population is 1 because of the selection adopted.

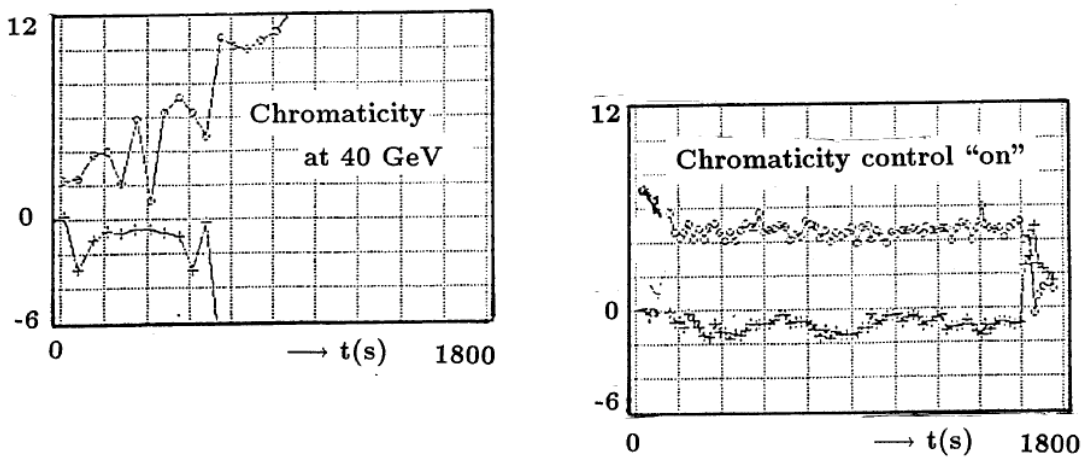

Figure 9. Chromaticity in the x and y plane during injection (a) without correction system and (b) with correction system active. Courtesy of B. Holzer [6].

Figure 9 (a) shows the effect of decaying persistent currents that lead to a change in the horizontal and vertical chromaticities in opposite directions [6], [7]. Without correction, the chromaticity reaches unacceptable values within few minutes. However, if the correction system is switched on, as shown in Fig. 9 (b), the use of reference magnet data counteracts the decaying persistent current sextupole fields

and the chromaticity in both planes is kept close to the desired values. As in the case of the Tevatron dipoles, these results show that a single magnet can be taken to represent the behaviour of a whole family.

Scaling law for the influence of powering cycles

The decay and snap-back of allowed multipoles in the LHC magnets is known to be strongly dependent on the powering history of the magnet [8]-[12]. The studies and analyses performed over short dipole models, dipole prototypes and series dipole magnets have concentrated on the measurement of decay and snap-back following a quench, erasing all previous memory, and a current cycle whose current values and duration have been varied parametrically. The prototype of this cycle is shown in Fig. 10, which also defines the main parameters varied.

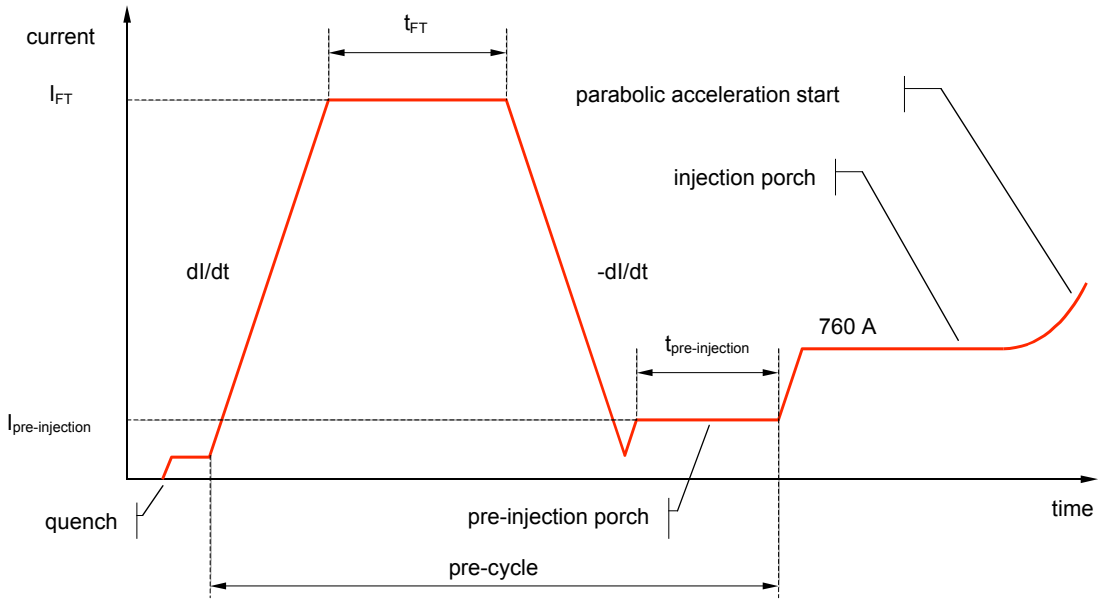

Figure 10. Prototype pre-cycle and definition of the main parameters defining its shape.

Variations of the pre-cycle affects the decay amplitude. In terms of the results reported in the previous section we describe this through a change in the parameter Δ_n in Eq. (1). Whether the dynamics of the decay is also affected, i.e. the value of the time constants τ_1 and τ_2, is so far still unclear. We assume that this is not the case. This assumption shall be verified through dedicated measurements.

The measurements cited above have shown that three parameters are the most important ones in determining the injection decay and subsequent snap-back are the flat-top current I_{FT}, the flat-top time t_{FT} and the time spent in the pre-injection porch $t_{pre\text{-}injection}$.

To model the changes in Δ_n we use the following parameterization:

$$\Delta_n = \Delta_n^{std}\left(\frac{I_{FT}}{I_{std}}\right)\left(\frac{A - Be^{-\frac{t_{FT}}{\tau}}}{A - Be^{-\frac{t_{std}}{\tau}}}\right)\left(\frac{C + De^{-\frac{t_{pre-injection}}{\tau}}}{C + D}\right) \quad (5)$$

where Δ_n^{std} is the decay measured for a standard pre-cycle, i.e. with flat-top current of I_{std}, flat-top time t_{std}, no pre-injection, $t_{pre\text{-}injection}$=0, and τ is a time constant for the magnet memory. Equation (5) is a direct consequence of the assumption of exponential decay during constant current excitation, i.e. Eq. (1), where only the longest time constant has been retained.

The parameterization was tested against the average of the flat-top current and flat-top time influences as measured on a total of 8 magnets, listed in Tab. 3. When testing the influence of one parameter (e.g. the flat-top current) the second parameter was held constant (e.g. the flat-top time) at the value corresponding to the standard pre-cycle. Note in addition that due to the long test time (each measurement requires a quench and a complete pre-cycle that last several hours), in several cases only the influence of one of the two parameters was measured. We concentrate on the analysis of the normal sextupole, for which the measurements are most reliable.

magnet	aperture		parameter	
	1	2	I_{FT}	t_{FT}
1004	x	x	x	x
1007	x	x	x	x
1010	x	x		x
1011	x	x		x
1012	x	x	x	x
1018	x	x		x
3007	x	x	x	x
3017	x	x	x	x

Table 3. Magnets considered in the analysis of the influence of powering history on decay and snap-back at injection

parameter	units	
τ	(s)	519
A	(-)	3.53
B	(-)	1.19
Δ_n^{std}	(units @ 17 mm)	1.79
fit σ	(units @ 17 mm)	0.08

Table 4. Parameters obtained fitting the model of Eq. (5) to the b_3 decay measured as a function of flat-top current and flat-top time variations from the population analyzed, assume to represent the behavior of the LHC.

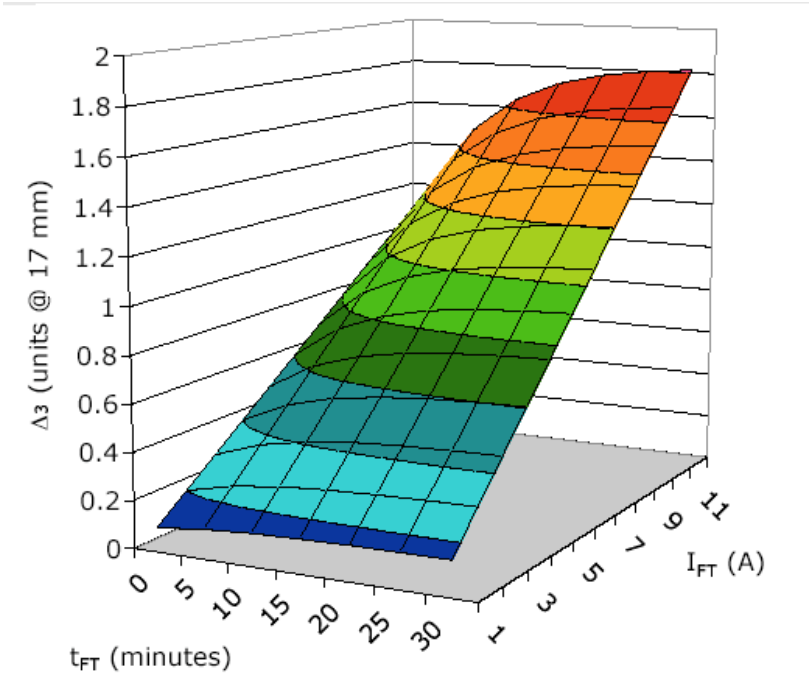

Figure 10. Plot of the surface of Δ_3 in the space defined by variations of the flat-top current and flat-top time, as generated with the parameters of Tab. 4 and representative for the LHC behavior.

The fit of the parameterization Eq. (5) gave the parameters reported in Tab. 4, and was found to produce an interpolation with a r.m.s. error of 0.08 units @ 17 mm at the measured points. The corresponding surface is shown in Fig. 11. Given the lack of data, it was not possible to parameterize the influence of the pre-injection waiting time, although this has been found to be very important, as also shown for the Tevatron dipoles [3].

As we have done for the dynamic of decay, we have now assumed that the linear scaling:

$$\left\langle \Delta_n^{std} \right\rangle = f_{decay} \ \Delta_{n,i}^{std} \tag{6}$$

can be used to deduce ring behavior from the measurement of a reference magnet. In this case $\left\langle \Delta_n^{std} \right\rangle$ is the average decay in standard powering conditions, while $\Delta_{n,i}^{std}$ is the decay of the reference magnet *i*. The scaling factor f_{decay} is given by the ratio of the average decay in the sample considered (e.g. sector or ring) and the decay of the reference magnet chosen. This is the same ratio as computed for the decay dynamics, through Eq. (4). Again, once the parameterization is fixed, the scaling has no free parameter.

We have finally used Eq. (5) with the parameters of Tab. 4 to compute the difference between the scaled behavior of a single magnet and the modeled average over the magnet population tested, that we assume as being representative of the whole ring. We have taken, as indicator of the quality, of the scaling the maximum error between the scaled magnet measurement and the population average. The result of this analysis is plotted in Fig. 12. The maximum error ranges from 0.07 to 0.3 units @ 17

mm, with an average value of 0.13 units @ 17 mm. We take this last value as representative for a reasonable choice of a reference magnet.

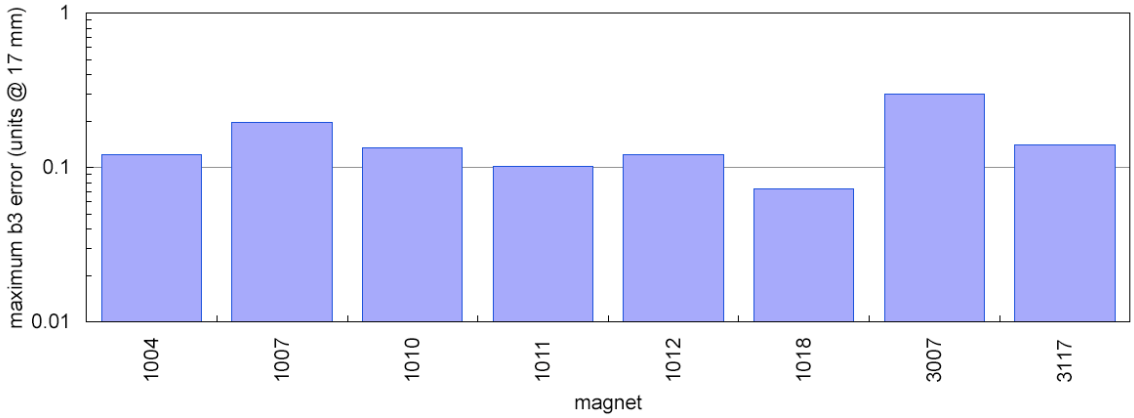

Figure 12. Maximum difference between the scaled sextupole decay factor Δ_3 and the average sextupole decay factor $\langle\Delta_3\rangle$ of the magnet set analyzed.

Scaling law for the snap-back

LHC dipoles

During the snap-back the first allowed harmonics b_3 and b_5 follow an exponential law of the type [13], [12]-[15]:

$$c_n^{snap-back}(t) = \Delta c_n e^{-\frac{I(t)-I_{injection}}{\Delta I}} \qquad (7)$$

where $c_n^{snap\text{-}back}(t)$ is the change of the harmonic during the snap-back, $I(t)$ is the instantaneous value of the current, initially at the injection value $I_{injection}$. The snap-back amplitude Δc_n and the current change ΔI are two fitting constants. The quality of the fit is generally better than 0.1 units on the maximum error during the whole snap-back. This is demonstrated in Fig. 13 for a typical measurement performed on the dipole 3005.

Given this good description, and once the fit parameters Δc_n and ΔI are known, the current (and hence time) dependence of the harmonic change during snap-back can be accurately described with this simple model. In fact, the parameter Δc_n is nothing else but the decay at the end of injection, and could be determined from the double exponential fit of Eq. (1).

Taking data on a single magnet for different magnet powering sequences, the fit parameters Δc_n and ΔI change, in accordance with the fact that the snap-back following the decay is a function of the magnet powering history. We observed however that the set of fit parameters obtained is strongly correlated, and once represented in a scatter plot Δc_n vs. ΔI they lie on a straight line, as shown in Fig. 14 for all dipoles tested to date at LHC. The implication is that only one of the two fit parameters, either Δc_n or ΔI, is strictly necessary to predict the sextupole change.

The most interesting property, however, is that the correlation between the fit parameters Δc_n and ΔI is the same (within the accuracy of the measurement and data analysis) in all magnets tested, also shown in Fig. 14. This fact suggests that the scatter plot representation adopted and the correlation found is an *invariant* property of a *magnet* design *family*, independent of the specific properties of each magnet instance.

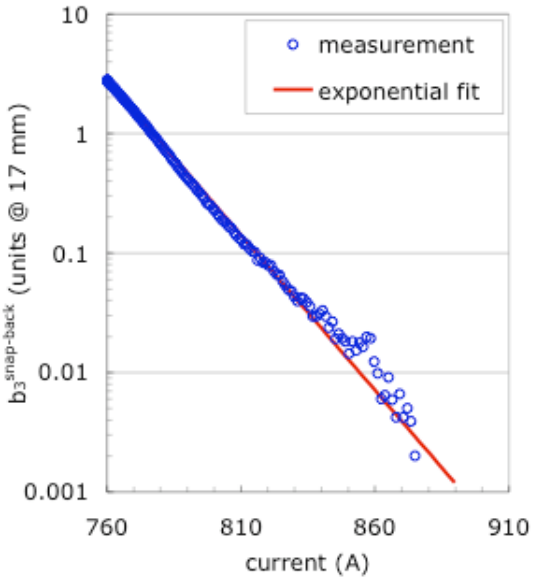

Figure 13. Exponential fit of measured sextupole change during snap-back on the LHC dipole 3005.

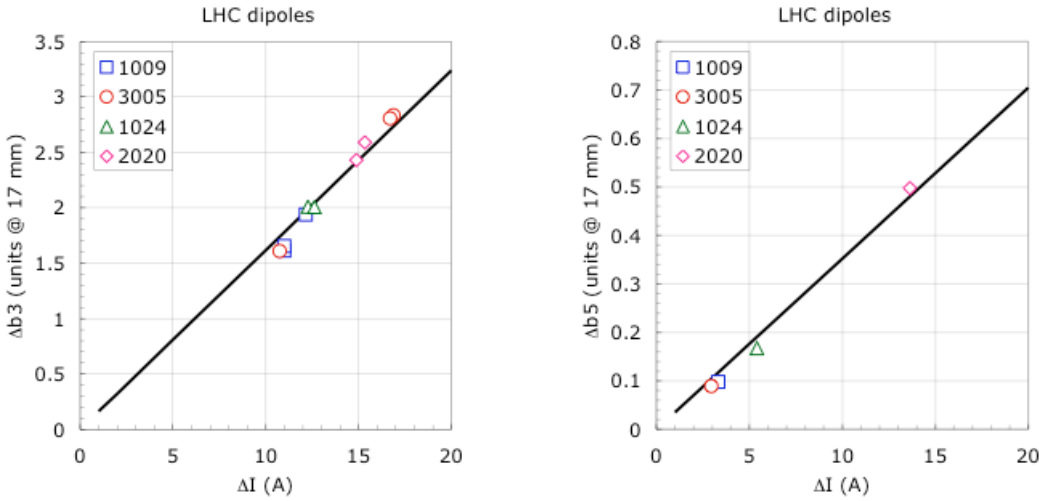

Figure 14. Scatter plot of the fit parameters Δc_n and ΔI that correspond to sets of different powering cycles in the four LHC dipoles tested and analyzed to date. Sextupole (left) and decapole (right) correlations are reported.

This postulate is substantiated by the fact that the magnets tested were not specially selected (e.g. with respect to cable properties) and comparable results are found performing the same measurements and data analysis on both the LHC and Tevatron

dipoles, as discussed later. Hence it seems that the correlation plot can be used to characterize the behavior of the dipoles in the whole accelerator, i.e. it can act as a scaling law.

In practice, the waveform of the snap-back can be predicted by taking the observed decay Δc_n at the end of injection (e.g. computed using Eq. (1)), and computing the corresponding ΔI using the linear correlation coefficient $f_{snap\text{-}back}$:

$$\Delta c_n = f_{snap-back} \Delta I \tag{8}$$

We have proceeded in this case as for the scaling analyses described above. We have taken in particular the maximum deviation of the fit parameter Δc_n, representing the amplitude of the snap-back, from the correlation Eq. (6) for all measurement sets analyzed. The maximum errors on the sextupole and decapole snap-back amplitudes are reported in Figs. 15 and 16 for all magnets tested. The errors for the sextupole range from 0.07 to 0.3 units @ 17 mm, with an average value of 0.08 units @ 17 mm. For the decapole the error are around 0.02 units @ 17 mm, with average in the same range.

We take the above values for the average error as an estimate for the deviation between the predicted and actual snap-back waveforms in the accelerator.

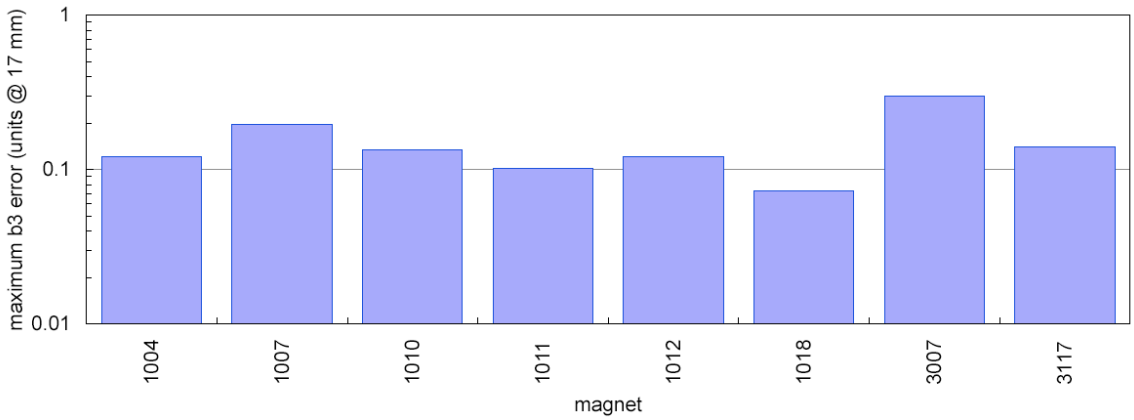

Figure 15. Maximum difference between the scaled sextupole snap-back amplitude factor Δc_3 and the factor predicted by the correlation Eq. (8) over the magnet set analysed.

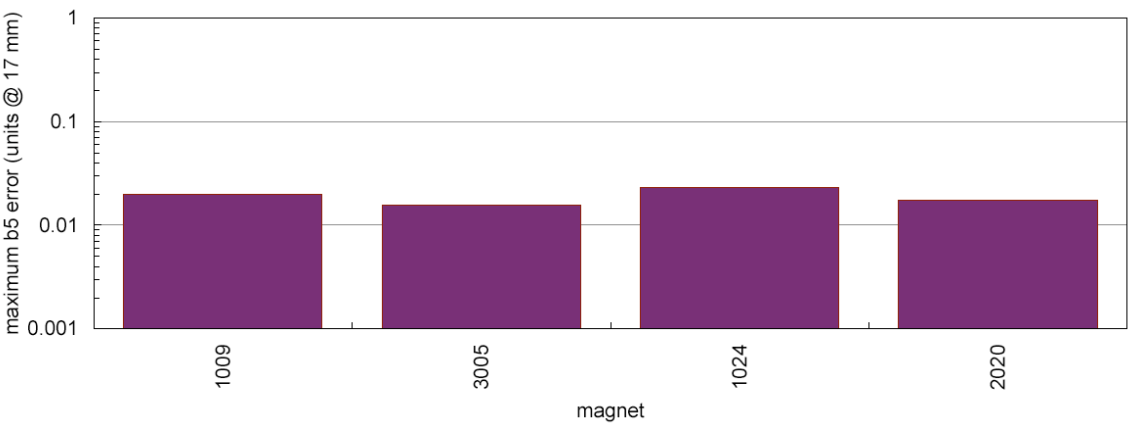

Figure 16. Maximum difference between the scaled decapole snap-back amplitude factor Δc_5 and the factor predicted by the correlation Eq. (8) over the magnet set analyzed.

Tevatron dipoles

Sextupole snap-back measurements of the same type as described above were performed to a great extent on four Tevatron dipoles. Following the same analysis procedure as for the LHC dipoles, the results can be represented in the same scatter plot as Fig. 14, and lead to the same conclusion, namely that the two parameters Δc_n and ΔI are strongly correlated. The results obtained are reported in Fig. 17, data have been obtained by courtesy of P. Bauer and G. Ambrosio, at FNAL.

The fact that we obtain the same result on two different families of dipole magnets, with major design and manufacturing differences (both on the superconducting cable and coil) supports the idea that the correlation found has some fundamental origin, and can thus be used for a robust prediction.

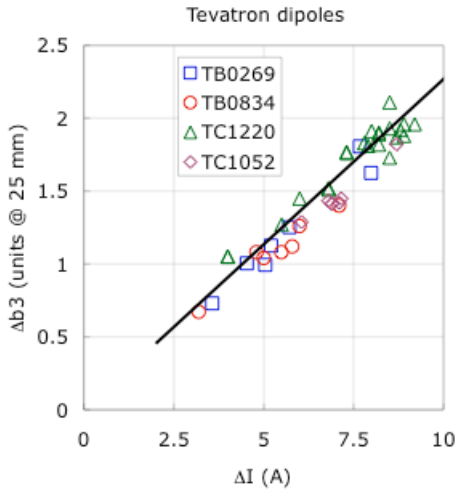

Figure 17. Scatter plot of the fit parameters Δb_3 and ΔI that correspond to sets of different powering cycles in four Tevatron dipoles tested and analyzed to date.

Discussion and conclusions

We have shown here that a set of simple scaling laws can be used to deduce the decay and snap-back behavior of a set of several magnets, representing a sector or the whole ring in the LHC, from measurements taken on selected magnets, i.e. reference magnets. As we have shown in the analysis, the error of the scaled predictions does not depend drastically on the magnet selected, so that the selection of a *good* reference magnet should not be a critical process. In practice, following the reasoning of this note, half of the magnets produced could be used as reference magnets.

In Tab. 5 we report a summary of the maximum expected errors during the decay, which is obtained as the quadratic sum of the error on the prediction of the cycle

dependency and the error on the dynamics, and during the snap-back. Most values for b_1 are missing due to the lack of reliable measurements at this level of analysis. For the sextupole, for which all entries in the summary are available, we see that a scaled reference magnet should represent a sector, or the whole ring (depending on the scaling applied) to within 0.15 units @ 17 mm during the injection porch, and 0.17 units during snap-back. These values correspond to 5 to 10 units of chromaticity.

To estimate the order of magnitude of the predictability of b_1 and b_5, for which some of the estimates are missing (due to lack of good data or good measurements) we can make the hypothesis that the ratios of the errors b_1/b_3 and b_5/b_3 stay constant. The ratio can be obtained from the analysis of the dynamics of the decay, for which the estimates are available on b_1, b_3 and b_5. If we proceed this way, we have that a scaled reference magnet is expected to represent the sector (or ring) average of b_1 to within 1.6 units @ 17 mm during the injection porch, and the b_5 average to within 0.06 units @ 17 mm. The snap-back is expected to be predictable to better than 2.4 unit @ 17 mm for b_1 and as well as 0.02 units @ 17 mm for b_5.

	Injection porch			Snap-back
	Decay dynamics	Powering cycles	Total	
b_1	0.9	*1.4*	1.6	*2.4*
b_3	0.08	0.13	0.15	0.17
b_5	0.03	*0.05*	0.06	0.06

Table 5. Summary of the maximum expected difference between predicted multipoles obtained scaling the measurements from a reference magnet, and the sector (or ring) average. The total values for the injection porch are obtained as the quadratic sum of the error in the prediction of pre-cycle effects and of the injection dynamics. Values in italic (red) are obtained scaling the b_3 estimate based on the ratio established from the analysis of the decay dynamics. All values in units @ 17 mm.

As a last word of caution, although orders of magnitude are discussed in this note, it seems to be early to give definite figures for predictability of decay and snap-back on all allowed multipoles. A significantly larger sample would be needed to confirm the results, in particular on the pre-cycle dependency, including the effect of pre-injection waiting time, and detailed snap-back waveform. In addition, b_1 changes should be mapped more precisely to allow more definite conclusions to be drawn, which implies a significant effort on the instrumentation.

6) References

[1] G. Annala, et al., Measurements of Geometric, Hysteretic and Dynamic Sextupole in Tevatron Dipoles, Fermilab/TD Report TD-04-043, November 2004.

[2] G. Annala, et al., Tevatron Chromaticity and Tune Drift and Snapback Studies Report, Fermilab/AD/TEV Report Beams-doc-1236, January 2005.

[3] G.V. Velev, Measurements of Sextupole Decay and Snapback in Tevatron Dipole Magnets, Proceedings of European Accelerator Conference, Lucerne, Switzerland, pp. 1780-1782, 2004.

[4] P. Bauer, et al., Proposals for Improvements of the Correction of Sextupole Dynamic Effects in Tevatron Dipole Magnets, Proceedings of European Accelerator Conference, Lucerne, Switzerland, pp. 818-820, 2004.

[5] H. Brueck, D. Degele, P. D. Gall, G. Hase, R. Meinke, M. Stolper, F. Willeke, Reference Magnets for the Superconducting HERA Proton Ring, Proceedings to the High Energy Accelerators Conference, vol 2, pp. 614-616 , Hamburg 1992.

[6] B. Holzer, Impact of Persistent Currents on Accelerator Performance, CERN Accelerator School (CAS), CERN 96-03, pg. 123, Hamburg Germany, May 1996.

[7] B. Holzer, C. Montag, Reproducibility and Predictability of persistent Current Effects in the HERA Proton Storage Ring, Proceedings to the European Accelerator Conference, Vienna Austria, pp. 2142-2144, 2000.

[8] M. Schneider, Decay and Snap-back Studies on the LHC Dipole Model Magnets. A Scaling Law, Ph.D. Dissertation, Technischen Universitaet Wien, 1999.

[9] L. Bottura, L. Walckiers, R. Wolf, Field Errors Decay and "Snap-Back" in LHC Model Dipoles, IEEE Trans. Appl Sup., **7** (2), pp. 602-605, 1997.

[10] M. Haverkamp, L. Bottura, M. Schneider, Studies of Decay and Snapback Effects on LHC Dipole Magnets, Proc. 4th European Conference on Applied Superconductivity, Sitges, Spain, Inst. Phys. Conf. Ser., **167**, pp. 1183-1186, 2000.

[11] M. Haverkamp, A. Kuijper., A. den Ouden, B. ten Haken, L. Bottura, H. ten Kate, Interaction between Current Imbalance and Magnetization in LHC Cables, IEEE Trans. Appl. Sup., **11** (1), pp. 1609-1612, 2001.

[12] M. Haverkamp, Decay and Snap-back in Superconducting Accelerator Magnets. A Scaling Law, Ph.D. Dissertation, Twente University, Enchede, 2003.

[13] S. Amet, L. Bottura, L. Deniau, L. Walckiers, The Multipoles Factory: an Element of the LHC Control, IEEE Trans. Appl. Sup., **12** (1), pp. 1417-1421, 2002.

[14] T. Pieloni, S. Sanfilippo, L. Bottura, M. Haverkamp, A. Tikhov, E. Effinger, E. Benedico, N. Smirnov, Field Decay and Snapback Measurements using a Fast Hall Probes Sensor, IEEE Trans. Appl. Sup., **14** (2), pp. 1822-1825, 2004.

[15] L. Bottura, T. Pieloni, S. Sanfilippo, G. Ambrosio, P. Bauer, Fermilab, M. Haverkamp, A Scaling Law for Predicting Snap-back in Superconducting Accelerator Magnets, Proceedings of European Accelerator Conference, Lucerne, Switzerland, pp. 1609-1611, 2004.